www.vbripress.com, www.amlett.com, DOI: 10.5185/amlett.indias.195
"INDIAS 2010" Special Issue Published online by the VBRI press in 2011

Assessing the conformational and cellular changes of ZnO nanoparticles impregnated *Escherichia coli* cells through molecular fingerprinting

Ranu K. Dutta*, Prashant K. Sharma, Avinash C. Pandey

Nanotechnology Application Centre, University of Allahabad, Allahabad 211002, India

*Corresponding author. Tel/Fax: (+91) 532 2460675; E-mail: ranu.dutta16@gmail.com

Received: 25 Dec 2010, Revised: 10 March 2011 and Accepted: 11 March 2011

ABSTRACT

Here is an insight into the effects of interaction of ZnO nanoparticles and the various cellular level changes that are brought about by the help of Raman spectroscopy on individual *Escherichia coli* cells. Raman vibrational signatures show variation in peak intensities of some of the cellular components of E coli cells with increase in nanoparticles concentration. This can be attributed to the cellular and molecular changes associated with bacterial cell growth, as the cells proceed from lag phase to stationary phase, which indicates that ZnO interferences with bacterial growth. Growth kinetics studies show mitigation in growth and colony forming units (CFU) counts. Changes in cellular morphology as investigated by atomic force microscopy and scanning electron microscopy, show destruction and even rupture of cell wall at higher ZnO concentration. This study pertains to any alterations brought about at the cellular level, which may be extended to other nanomaterials in the environment and the effect on human cells as well.

Keywords: Bactericidal effect; Raman spectroscopy; AFM; ESEM; ROS.

Ranu K. Dutta completed her B.Sc. in 2005 from Andhra University and Masters in Biotechnology in the year 2007 from University of Allahabad, India. Since Oct 2007, she is at the Nanotechnology Application Centre (formerly Nanophosphor Application Centre), University of Allahabad, India, as a D.Phil. student. Presently she is working as Research Scientist at Nanotechnology Application Centre, University of Allahabad, India. Her area of research includes identification and optimization of the synthesis methods for the highly efficient bare & doped nanophosphors with and without capping and determination of the corresponding functional properties in view of biomedical applications. During this period she has published more than 16 papers in the refereed international Journals and 6 Patents to her credit.

Prashant K. Sharma completed his B.Sc. in 2004 and Masters in Physics in the year 2006 from University of Allahabad, India. Since May 2006, he is at the Nanotechnology Application Centre (formerly Nanophosphor Application Centre), University of Allahabad, India, as a D.Phil. student. Presently he is working as Research Scientist at Nanotechnology Application Centre, University of Allahabad, Allahabad, India. His area of research includes, identification and optimization of the synthesis methods for the highly efficient bare & doped nanophosphors with and without capping and determination of the corresponding functional properties in view of efficient LEDs, Opto-electronic, PDP and biomedical applications. Mr Sharma has expertise of wide range of material characterization techniques, especially Microscopic and Spectroscopic techniques. During this period he has published more than 40 papers in the refereed international Journals and 8 Patents to his credit.

Avinash C. Pandey holds four masters degrees namely M.Sc. (Physics, 1984), MBA (Marketing, 1993) and M.Sc. (Mathematics, 1996) from University of Allahabad, India and M. Tech.(Computer Science) from Motilal Nehru National Institute of Technology, India. He did his D. Phil. from University of Allahabad in the year 1995. He joined University of Allahabad in the Department of Physics as Assistant Professor and is now Professor and Head of Department of Atmospheric & Ocean Studies. He is the Principal Investigator and co-ordinator of Nanotechnology Application Centre, K. Banerjee Centre of Atmospheric & Ocean Studies. He is also Principal Investigator in more than 20 externally funded research projects worth of multi crore at K. Banerjee Centre of Atmospheric & Ocean Studies, M. N. Saha Centre of Space Studies and Nanotechnology Application Centre. He has built up two district groups at University of Allahabad dealing with various aspects of synthesis and characterization of Nanomaterials for their applications in Solid State Lighting, Display Technology and Nano-medicine and Mathematical Modeling of Atmosphere and Ocean. Prof. Pandey has made outstanding contributions to the basic understanding of quantum confined atoms and their applications in

several devices. He has introduced well recognized innovations in experimental techniques for nanostructuring research. He has promoted growth of user facility and capacity building in front ranking areas by developing state-of-art facility through project funding. He has been also involved with industrial research for over 10 years including development of opto-electronics such as LEDs, medical research, electronic materials, optical recording and nanotechnology In 2004, he established Nanotechnology Application Centre to develop application of nanophosphor and other nanomaterials in the field of lighting imaging and displays. Prof. Pandey has guided 12 PhD students and is presently supervising 10 doctoral students and mentoring 6 post-docs. His area of research includes ion beam techniques, Nanomaterial Synthesis and processing by ion beams and wet chemistry, bare & doped nanophosphors with and without capping and determination of the corresponding functional properties in view of efficient LEDs, Opto-electronic, PDP and biomedical applications. To his credit, he has authored more than 150 scientific papers in different International journals, 10 book chapters and monograms and 12 patents in the field of opto-electronics and Nanomedicines. He is an Associate of Abdus Salam International Centre of Theoretical Physics (ICTP), Trieste, Italy and the member of many professional bodies.

Introduction

Nanometer scale composites having multifunctional properties display unique, superior and indispensable properties and have attracted tremendous attention for their distinct characteristics that are unavailable in conventional macroscopic materials. In the recent years much attention has been paid to the synthesis, characterization and applications of these nanoparticles due to their excellent unique size dependent properties **[1-3]**. Quantum dots **[4]** such as ZnO **[5]**, TiO_2 **[6]**, CdS, CdSe, CdTe, CdSe@ZnS and carbon nanotubes are widely used in light-emitting devices **[7, 8]**, diluted magnetic semiconductors (DMS) **[9 -12]**, display devices, photo detectors, photodiodes, transparent UV protection films, biological systems **[13]** (drug delivery system, bio imaging, *in vivo* cell imaging etc.), cosmetic products and chemical sensors. With the increased prevalence of nanoparticles in commercial products like cosmetics and sunscreens (TiO_2, Fe_3O_4, and ZnO) **[14]**, fillers in dental fillings (SiO_2), in water filtration and catalytic systems, photovoltaic cells (CdS, CdSe, ZnS) etc, a public debate is emerging on the toxicological and environmental effects of direct and indirect exposure to these airborne nanosized particles **[15]**. While beneficial aspects of nanomaterials are well visualized, several reports have reminded the harmful impact of nanomaterials on living cells. The process of bioaccumulation and biomagnifications may be the consequence of the ignorant use of nanoparticles in the environment. The disruption may even be carried as mutation in the genome and pass on subsequently.

Many studies on the biological activity of ZnO have been carried out; most of these pertain to the antimicrobial effect of bulk ZnO with a large particle size. Cellular damage caused by ZnO can be attributed to the Size (Yamamoto *et al*. **[16]**), shape, roughness or orientation of ZnO (Wang *et al* **[17]**). They are known to damage cells by the production of Reactive Oxygen Species (ROS) inside cells. Analyzing the effects of nanoparticle's interaction with biological cells or characterizing molecular interactions in the biological cell is currently a challenging task. Since the emergence of nanotechnology, studies pertaining to the toxicological impact of nanoparticles as determined by growth curve, scanning electron microscopy (SEM), transmission electron microscopy (TEM) are abundant in literature. An exact molecular mechanism remains to be elucidated for the precise molecular and cellular level changes that are infested by nanoparticles inside individual living cells. Proper cell signaling mechanism is not yet properly understood. Nanoparticles have large surface to volume ratio which increases their reactivity towards biomolecules. Here is an insight into the preliminary study of a more precise molecular level changes of bacterial cells brought about by nanoparticles. Besides carrying out the growth kinetics and morphological studies, we have used Raman Microscopy as a tool to study the change in vibrational signatures in some of the cellular components of *Escherichia coli* cells upon ZnO exposure. Along with atomic force microscopy (AFM), the Raman microscopy enables us to determine the interaction of different microorganisms and other substances with nanoparticles.

Raman spectra are obtained from each position in a sample, and the distribution of intensity of Raman scattering is used to construct an image of a molecular distribution. Raman peak in the spectrum can be assigned to molecular vibrations of chemical bonds in the sample by measuring the inelastically scattered light following excitation. Biologically associated molecules such as nucleic acids, protein, lipids, and carbohydrates all generate strong signals in Raman spectra. The exploitation of a Raman microscope allows us to determine the three-dimensional distribution of substances with high spatial resolution by scanning a tightly focused laser beam over the sample. Raman spectroscopy can tolerate water molecules and can generate more sharp and distinguishable bands of specific molecules. Therefore, the Raman spectroscopic method can be used to generate "whole-organism fingerprints" for the differentiation of biological samples or in analyzing the effect of nanoparticles' interactions with biological cells or characterizing molecular interactions in the biological cell. In past, some researchers **[18-24]** showed Raman spectroscopy as an effective tool for the rapid identification of bacteria, fungi and for the study of the mode of action of antibiotics **[25]**. While, the chemotaxonomic identification of single bacteria by micro-Raman spectroscopy was studied by Rosch *et al.* **[26]**.

In the present work, *Escherichia coli* cells were treated with a range of ZnO concentrations between 0μg/ml to 100μg/ml. The changes in growth kinetics were studied by measuring the optical density of the cells in the growth medium, represented by growth curves and estimation of CFU (Colony Forming Unit) counts. OD is a simple method to evaluate the cytotoxicity of the material and CFU count is a measure of the ability of bacteria to replicate. Optical density of the growth medium and CFU counts decreased in comparison to the control with increasing concentration of ZnO nanoparticles. Changes in cellular morphologies were studied by AFM and SEM analysis, which show cell wall destruction and damage at higher ZnO concentration and probably death of the cells at the highest concentration. Besides this, we have prognosticated the probable cellular level changes infested on cells after interaction with ZnO by Raman microscopy by the specific Raman vibrational signatures originated from the cellular components like DNA, proteins, lipids etc. The presented

results provide new insights into the study of interaction between ZnO nanoparticles and *Escherichia coli* cells.

Experimental

We used, the ZnO nanoparticles (having mean size 15 nm) synthesized by our group **[27]**, to study the bactericidal effect of these ZnO nanoparticles on the *Escherichia coli* cells.

Optical density and growth kinetics estimation

The optical density of ZnO treated *E coli* cells was recorded using Perkin Elmer Lambda 35 UV-Visible spectrometer. The density of bacterial cells in the liquid cultures was estimated by O. D measurements at 600 nm.

Environmental scanning electron microscopy analysis

The effect of interaction of ZnO nanomaterial with *E coli* cells were observed with a scanning electron microscope model Quanta 200 MK2 microscope operated at 25 kV in Environmental SEM (ESEM) mode on the ZnO treated *E coli* films.

Atomic force microscopy analysis

An atomic force microscope (AFM) model Nanonics Multi-view 2000 having piezo-electric scanner's with < 0.005 nm (Z), < 0.015 nm (XY), < 0.002 nm (XY) low voltage mode resolutions was used to investigate the surface topography of the bacterial samples. The obtained AFM images were processed on WSxM 4.0 software to determine the surface roughness and distance vs height curves.

Raman analysis

Raman spectra were recorded on a Renishaw make micro - Raman (model RM-2000) integrated with Nanonics AFM (model Multiview 2000, capable of ~ 2 λ spatial resolution. 514 nm Ar^+ laser was used as excitation source. Typically, the incident laser power was attenuated to 2 mW and acquisition time was set to 50 S throughout the measurements. This Raman microscope was equipped with an integrated Leica microscope having three distinct microscope objectives as 5×, 20× and 100× respectively. In the current work all the Raman data were acquired with 100× objective. The detector used was a Peltier air-cooled CCD detector. The true performance of the instrument allows the analysis of single cells of 1μm or smaller size. The laser beam was targeted on the single bacterial cell visually in videoscope mode on computer screen, using 100 × objective. Raman signal was optimized by adjusting the laser focus; the full range spectrum (100 cm^{-1} – 3200 cm^{-1}) were recorded for glass slide, bacterial growth media, untreated *E coli* cells, *E coli* cells treated with 20μg/ml ZnO, 40μg/ml ZnO, 60μg/ml ZnO 80μg/ml ZnO, 100μg/ml ZnO and only ZnO nanoparticles. Furthermore, the spectra between 800–2000 cm^{-1} range were again recorded for precise estimation of several cellular components. The system was calibrated, prior to analysis, and monitored using a silicon Raman band reference.

Bacterial culture

Bacterial culture *Escherichia coli* (DH 5α) were obtained from Centre for Cellular and Molecular Biology (CCMB), Hyderabad, India. Agar, Yeast extract, Peptone and NaCl were purchased from Alfa Aesar, Germany and were of bacteriological grade. The axenic culture of *E coli* (DH5α) was grown in liquid nutrient broth medium containing NaCl (5 g), peptone (5 g) and yeast extract (2.5 g) in 100ml water. The density of bacterial cells in the liquid culture was estimated by optical density (O. D.) measurements at 600 nm and was maintained at 0.8 - 1.0, which is the ideal optical density of the cells. ZnO nanoparticles were dispersed in autoclaved deionized water by ultrasonication to prepare a stock solution. For our experimental investigation, E. coli culture (50 μl) with an approximate concentration of 10^6 colony forming units per milliliter (CFU/ml) was inoculated to a series of 50 ml media containing a range of ZnO nanoparticle concentrations between 20μg/ml - 100μg/ml and incubated at 37˚C with constant shaking. One sample was taken as a control, with no nanoparticle load. In liquid medium, the growth of *E coli* was indexed by measuring O. D at 600 nm against abiotic control after every 2 h up to 24 h. OD is a simple method to evaluate the cytotoxicity of the material. After 24 h, cell viability was measured by serial dilution of the culture in sterile distilled water. The viable cell number was recorded by counting the number of bacterial colonies grown on the plate multiplied by the dilution factor and expressed as CFU/ml.

Sample preparation for microscopic analysis

The direct analysis of bacterial cells from colonies growing on the culture medium minimizes sample preparation and time. However, the major problem with this approach can be the result of any (or combination of) the following: limited thickness of the microcolony, the focal point, and the Raman signal not only originating from the colony, but beyond the depth resolution, from the culture medium. Thus, the resultant Raman signal consists of signal contributions not only from the bacterial cell but also from the underlying culture medium. In order to overcome this difficulty, the samples were washed prior to analysis. These sample were taken from the stationary phase of the bacterial growth. About 3 ml of culture from each of the samples were centrifuged at 3000rpm for 5 minutes and cells were washed with sterile distilled water and suspended in 1 ml sterile distilled water. ~ 0.01 ml of bacterial cells from each washed sample was spread onto glass slides and allowed to dry prior to ESEM, AFM and Raman Spectroscopic analysis.

Results and discussion

Growth kinetics

Bactericidal effect of ZnO nanoparticles was studied against the Gram-negative bacteria *E. coli* (DH5α). Bacterial cells grow by a process called binary fission in which one cell doubles in size and splits into halves to produce two identical daughter cells. Bacterial cell growth

enhances the turbidity of the liquid nutrient medium and as a result the absorption increases. Optical densities as a function of time measured periodically up to 24 h of the control and solutions containing different concentrations of ZnO nanoparticles treated *E. coli* are shown in **Fig. 1**. In our experiment (**Fig. 1a**), slope of the growth curve continuously decreases with increasing nanoparticle concentration from 0 to 100 µg/ml. The kinetics of bacterial growth was found ZnO dose dependent and the number of bacteria required to reach the stationary phase of growth decreases. This is evident from the reduction in the OD from 0.6 of the control to 0.06 of the culture containing 80 µg/ml of ZnO, i.e. almost 10 times reduction in OD was observed. At the highest concentration, almost negligible growth and a clear flattening of the growth curve and complete absence of exponential phase was observed. Hence disruption of the DNA synthesis may have been caused with increase in nanophosphor concentration.

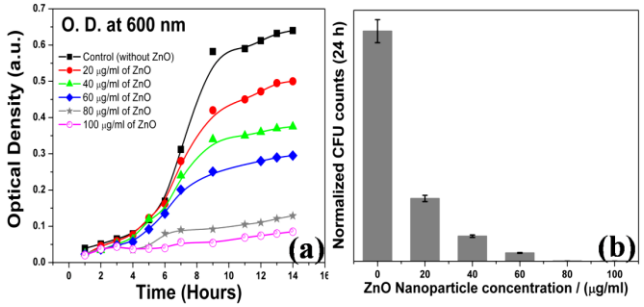

Fig. 1. (a) Growth curve: Optical density as function of time with varying concentration of ZnO nanoparticles treated *E coli* in solution state. (b) Antibacterial characterization: CFU after 24 hour incubation time with varying concentration of ZnO nanoparticles on solid agar plates (error bar 5 %).

It has been observed that optical density of the growth medium decreased in comparison to the control with increasing concentration of ZnO nanoparticles. This has been attributed to the reduced growth of bacterial cells. The Growth curve [**Fig. 1 (a)**] shows mitigation of growth gradually from 20µg/ml to 80µg/ml and almost complete inhibition of bacterial growth at concentration of 100µg/ml. **Fig. 1 (b)** shows the normalized number of bacterial colonies grown on nutrient agar plates as a function of concentration of ZnO nanoparticles. The bacterial cell colonies on agar-plates were detected by viable cell counts. Viable cell counts are the counted number of colonies that are developed after a sample has been diluted and spread over the surface of a nutrient medium solidified with agar and contained in a petri dish. The number of CFU reduced significantly with increasing the concentration of ZnO nanoparticles, there was virtually no CFU observed in the samples containing 80µg/ml and higher ZnO nanoparticles. The bacterial growth inhibition trend observed from CFU data are in accordance with the results of optical density. Both MIC and MBC were calculated and found between 80 µg/ml -100 µg/ml and 100 µg/ml -120 µg/ml.

AFM and ESEM studies

Surface features and shape of *E coli* cells treated with different concentrations of ZnO nanoparticles were observed by AFM and ESEM measurements. **Fig. 2** shows the representative AFM images for the films of **(a)** *E coli* cells without ZnO treatment i.e. Control **(b)** *E coli* cells treated with 40µg /ml of ZnO nanoparticles **(c)** *E coli* cells treated with 100µg /ml of ZnO nanoparticles. Moreover the roughness profile and distance vs height curve were obtained by processing these AFM images on WSxM 4.0 software.

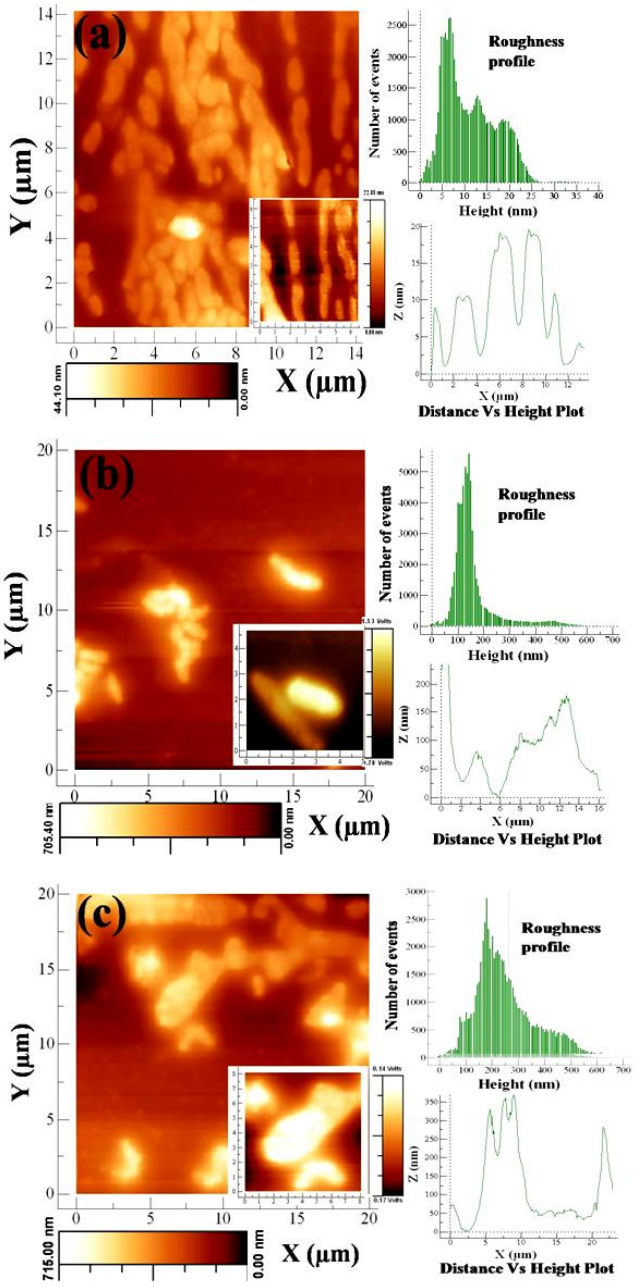

Fig. 2. AFM images (a) Control *E coli* films (i.e. *E coli* cells without ZnO treatment) (b) *E coli* films (*E coli* cells treated with 40µg /ml of ZnO nanoparticles) (c) *E coli* films (*E coli* cells treated with 100µg /ml of ZnO nanoparticles).

Initially bacteria maintained the hydrated appearance with no evidence of cell wall collapse [**Fig. 2 (a)**]. Later on, as we go on increasing the ZnO nanoparticle concentration, the bacteria start showing the dehydrated appearance with some evidence of cell wall collapse [**Fig. 2 (b)**]. For the maximum ZnO nanoparticle treated bacterial cells, strong

evidence of dehydration and cell wall collapse [**Fig. 2 (c)**] was observed. The differences in the bacterial packing density in AFM images can be attributed due to differences in the concentration of the spotted cultures. In higher resolution images, insets of **Fig. 2**, bacterial surface showed much rough surface with clear indication of damage caused [i.e. distortion of cell wall in **Fig. 2 (c)**] due to treatment of 100 µg/ml of ZnO nanoparticles. This is clearly evident from the roughness profile, distance vs. height curve as shown in **Fig. 2**. Greater roughness was observed for bacterial cells treated with higher concentration of ZnO nanoparticles and gives clear indication of damage caused on the surface of the bacterial cells due to increasing doses of ZnO nanoparticles. Similar results were observed from the ESEM analysis.

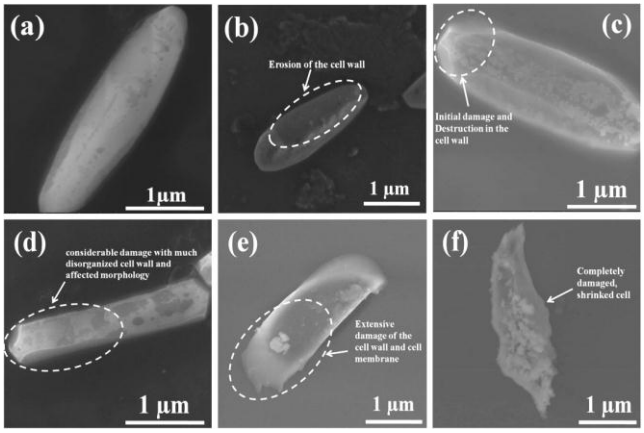

Fig. 3. ESEM micrograph of *E coli* treated with (a) Control i.e. without ZnO: showing an intact *E coli* cell, (b) 20 µg/ml ZnO: showing erosion of the cell wall of *E coli* cell, (c) 40 µg/ml ZnO: initial damage and destruction in the cell wall was observed, (d) 60 µg/ml ZnO: considerable damage with much disorganized cell wall and affected morphology was observed, (e) 80 µg/ml ZnO: Extensive damage of the cell wall and cell membrane was observed (f) 100 µg/ml ZnO: shrinked *E coli* cell membrane and probably cell death.

Fig. 3 shows ESEM micrograph of *E coli* cells **(a)** without ZnO: showing an intact cell, treated with **(b)** 20 µg/ml ZnO: showing erosion of the cell wall of *E coli* cell, **(c)** 40 µg/ml ZnO: initial damage and destruction in the cell wall was observed, **(d)** 60 µg/ml ZnO: considerable damage with much disorganized cell wall and affected morphology was observed, **(e)** 80 µg/ml ZnO: Extensive damage of the cell wall and probably cell membrane **(f)** 100 µg/ml ZnO: shrinked *E coli* cell membrane and probably cell death. For 80 µg/ml and 100 µg/ml concentrations of ZnO, the *E coli* cell morphology is extensively damaged (**Fig. 3 (e)** and **Fig. 3 (f)**) and it is likely that the intracellular content has leaked out hence shrinkage of cell (**Fig. 3 (f)**) and probably cell death has occurred. Preliminary results of cellular internalization of ZnO nanoparticles and cell wall disorganization have already been shown by Brayner *et al.* **[28]**. Brayner *et al.* showed *E coli* cells with damaged morphology at lower ZnO concentration and cell rupture at higher concentrations due to internalization of ZnO nanoparticles.

Raman spectroscopic studies

The bacterial cells at different growth phases will contain different bio-molecules and are expected to generate different Raman spectral signatures **[29, 30]**. The relatively short range (800 cm^{-1}- 2000 cm^{-1}) Raman spectra of selected single bacterial cell from each sample are shown in **Fig. 4**. This figure depicts *E coli* treated with **(a)** Control i.e. without ZnO **(b)** 20µg/ml ZnO (c) 40µg/ml ZnO **(d)** 60µg/ml ZnO **(e)** 80µg/ml ZnO and (f) 100µg/ml ZnO. For control i.e. untreated *E coli* cells Raman Spectra showed the main vibrational bands at 874, 961, 1006, 1126, 1157, 1199, 1216, 1271, 1296, 1313, 1355, 1452, 1516, 1586 and 1660 cm^{-1} [**Fig. 4(a)**]. Some of the major bands observed by us can be associated with nucleic acids **[31]** (1516, 1586 cm^{-1}) and aromatic amino acid **[22]** (1006 cm^{-1}). According to some authors **[32]**, the peak at 1516 cm^{-1} is also considered for aromatic amino acids. We do see an intense band at 1157cm^{-1} associated to protein **[23, 33]** (C-N, C-C stretching). Peak at 1126 cm^{-1} can be associated with C-N, C-C stretching **[34, 35]**. Raman band at 1452 cm^{-1} is due to presence of lipids **[34, 36]** (CH_2 deformation). For samples treated with 20µg/ml ZnO and 40g/ml ZnO, **Fig. 4 (b)** and **Fig. 4 (c)** respectively, almost all the Raman signals of *E coli* were present with slight variations in intensities.

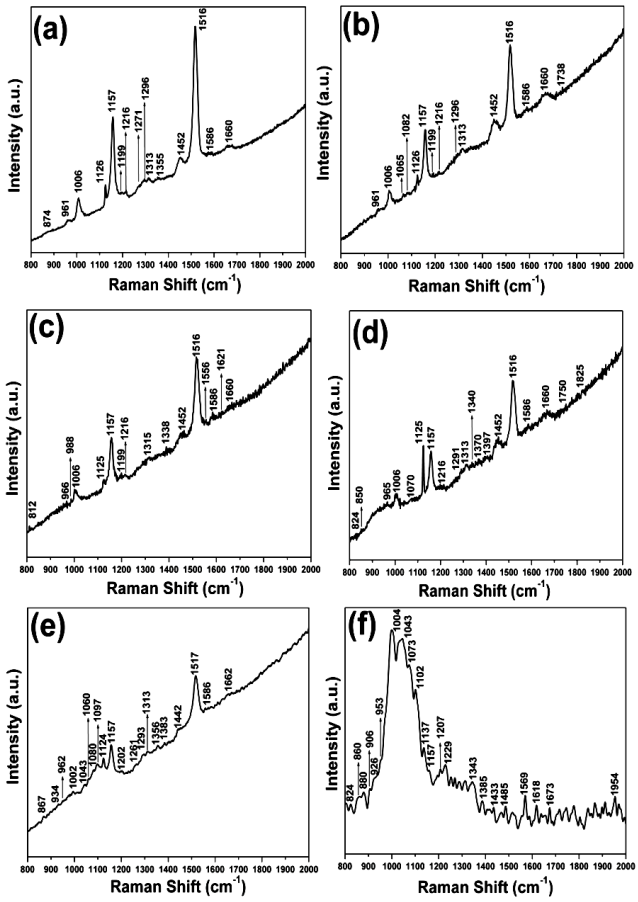

Fig. 4. Narrow range confocal Raman spectra of *E coli* treated with (a) Control i.e. without ZnO (b) 20µg/ml ZnO (c) 40µg/ml ZnO (d) 60µg/ml ZnO (e) 80µg/ml ZnO (f) 100µg/ml ZnO.

Furthermore, the representative full range Raman spectra are shown in **Fig. 4**, Supporting Information. **Fig. 4**, Supporting Information, show Raman spectra of (a) bare glass slide, (b) bacterial growth medium, (c) *E coli* cells without ZnO treatment i.e. Control (d) *E coli* bacterial cells treated with 40μg/ml ZnO (e) *E coli* bacterial cells treated with 80μg/ml ZnO and (f) only ZnO nanoparticles. The observed high background Raman scattering with no significant Raman signal in glass slide (**Fig 4 a**) can be attributed to the strong fluorescence under 514 nm visible laser excitation. The broad Raman signals at 450 and 930 cm^{-1} in **Fig. 4 (b)** is due to presence of protein in the growth media, whereas, the well known LO and TO optical phonon modes of ZnO were observed in **Fig. 4 (f)**. Besides this, the Raman signal corresponding to CH aliphatic chain around 3000 cm^{-1} was also observed for all the ZnO treated *E coli* cells (**Fig. 4 c, d, e**) and becoming weaker gradually with the increasing ZnO concentration, indicating damage of the cell wall components.

The most prominent Raman signal of *E coli* cell was at 1516 cm^{-1}. A clear suppression in this signal was observed with increasing concentration of ZnO nanoparticles and drastic reduction in this signal was observed for highest concentration of ZnO treated *E coli* cells. This shows reduction in nucleic acid content of the cells with increasing concentration of ZnO due to inhibition of DNA replication of bacterial cells. This can be supported by the growth curve analysis. Exponential phase is characterized by cell doubling which certainly pertains to the replication of DNA. The number of new bacteria appearing per unit time is proportional to the present population. If growth is not limited, doubling will continue at a constant rate so both the number of cells and the rate of population increase doubles with each consecutive time period. For this type of exponential growth, plotting the natural logarithm of cell number against time produces a straight line. The slope of this line is the specific growth rate of the organism, which is a measure of the number of divisions per cell per unit time. The actual rate of this growth depends upon the growth conditions, which affect the frequency of cell division events and the probability of both daughter cells surviving. In our experiment (**Fig. 1a**), slope of the growth curve continuously decreases with increasing nanoparticle concentration from 0 to 100 μg/ml. The kinetics of bacterial growth was found ZnO dose dependent and the number of bacteria required to reach the stationary phase of growth decreases. This is evident from the reduction in the OD from the control 0.6 OD to 0.06 OD of 80 μg/ml of ZnO, i.e. almost 10 times reduction in OD was observed. At the highest concentration, almost negligible growth and a clear flattening of the growth curve and complete absence of exponential phase was observed. Hence disruption of the DNA synthesis may have been caused with increase in nanophosphor concentration. This supports the explanation given for the mitigation in signal at 1516 cm^{-1}.This could be due to inhibition of DNA replication. The attainment of the stationary phase is clearly evidenced earlier with the gradual increase in nanoparticles concentration. Our results also showed peak at 961 cm^{-1} and according to Spiro and Gaber **[37]** this peak is due to the C-C stretch (or C-C-N stretch) for various proteins that are present in the cell wall. These peaks broaden and lose intensity with denaturation. The gradual broadening of peak (with decrease in intensity) can be attributed to some deformation of cell wall components with increase in ZnO concentration. Raman peak at around 1450 cm^{-1} can be assigned to the bending vibration mode of CH_2 which is contained in large amounts in the hydrocarbon chains of lipid molecules. Reduction in intensity may pertain to some cell membrane disruption caused at higher ZnO concentration, since lipids are abundant in the cell membrane of gram negative bacteria. Raman signal at 1680 cm^{-1} can be assigned to Amide-I vibrational mode of peptide bonds that can be commonly seen in proteins. This can be attributed to attenuation in coupled transcription and translation mechanism of *Escherichia coli* cells. For highest concentration of ZnO [**Fig. 4 (f)**], some overlapped Raman signal associated with second order ZnO vibrations were also observed between 990 – 1200 cm^{-1}. Broadening around 1000 –1200 cm^{-1} in Raman spectra was observed with maxima at 1004 cm^{-1} at the highest concentration of ZnO nanoparticle (100μg/ml ZnO). Peaks present in these regions are conformational markers and they broaden and decrease in intensity with denaturation of cellular components. This is an investigation of molecular dynamics in cells under oxidative stress. Some distinct peaks are seen as side bands, which may be due to different methods of sample preparation, measurement and some possible conformational changes of cellular proteins on interaction with increasing concentration of ZnO. Characteristic peaks determined from literature for cellular components such as carbohydrates, lipids, proteins and nucleic acids are present. Emergence of few different peaks seems to be due to the incorporation of ZnO nanoparticles.

We propose that the relevant mechanism in our case is membrane dysfunction owing to the interaction of ZnO with the cell membrane. This is supported by the fact that since ZnO particles, have been prepared in nonaqueous medium (i.e., methanol) it leads to oxygen deficient (Zinc rich) surface. This could exhibit a strong electrostatic interaction with the negatively charged cell membrane of the bacterial cells.

Several explanations have been given for the damage caused by ZnO on *E coli* cells. Brayner *et al* have reported the internalization of ZnO inside *E coli* cells causing triple membrane disorganization. Several other groups **[38-41]** have reported the interaction of ZnO with various cellular components causing DNA damage and oxidative lesions. ZnO is known to effect cell viability and damage DNA **[42].** Smaller size ZnO has higher antibacterial activity as determined by N Padmavathy and R Vijayaraghavan **[43]**.
One explanation is based on the reactive oxygen species released on the surface of ZnO, which cause fatal damage to the cells **[44]**. Generation of highly reactive oxygen species such as OH^-, H_2O_2 and O_2^{2-} can be explained as, ZnO with defects can be activated by both UV and visible light, which can create electron-hole pairs (e^- - h^+). The holes split H_2O molecules (from the suspension of ZnO) into OH^- and H^+. Dissolved oxygen molecules are transformed to superoxide radical anions ($^{\bullet}O^{-2}$), which in turn react with H^+ to generate ($HO_2^{\bullet}$) radicals, which upon subsequent collision with electrons produce hydrogen peroxide anions (HO_2^-). Then, they react with hydrogen ions to produce molecules of H_2O_2. The generated H_2O_2

can penetrate the cell membrane, causing destruction of lipids, proteins and DNA, thereby resulting in the bacterial **[45]** cell death. The schematic representation of reactive oxygen species (ROS) mediated cellular damage is shown in **Fig. 5**.The results obtained by Raman spectra are in accordance with the results obtained by AFM and ESEM investigations.

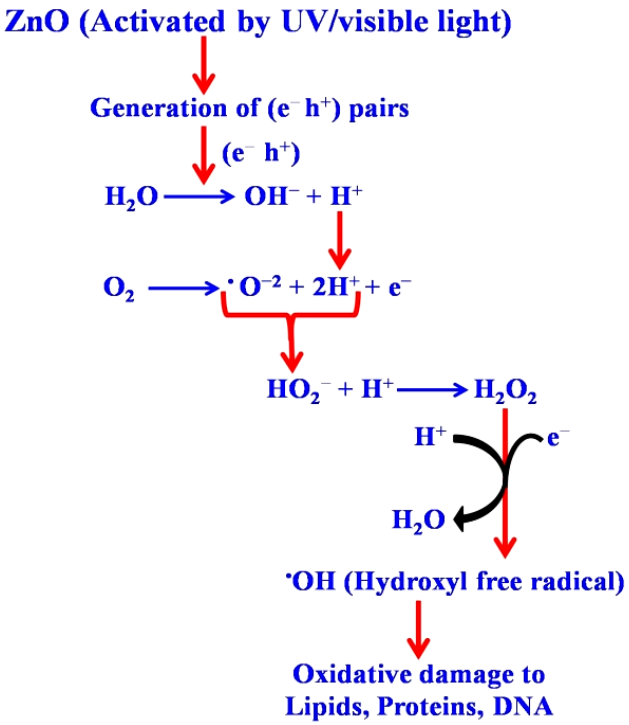

Fig. 5. Schematic representation of Reactive Oxygen Species (ROS) mediated cellular damage.

Conclusion

We are successful in precise assess and demonstration of the conformational and cellular changes in *E coli* bacterial cell due to presence of ZnO nanoparticles. The preliminary studies like the growth curve and CFU are well in accordance with the AFM, ESEM and Raman studies. The Atomic force microscopy (AFM) and environmental scanning electron microscopy (ESEM) studies showed distorted morphology at lower ZnO concentration and greater damage and even cellular death at higher ZnO concentration. Furthermore, Raman spectroscopy (CRS) enabled us to precisely analyze the effects of the interaction of *E coli* cell with the increasing concentration of ZnO nanoparticle by the variations in Raman signatures, through the reduction in signals on depletion of cellular components. Biological molecules such as nucleic acids, protein, lipids, and carbohydrates all generate specific Raman spectra, which provide biochemical information regarding the molecular composition, structure and interactions of nanoparticle in cells. This study pertains to the alterations in molecular components brought about at the cellular level, which may be extended to other nanomaterials in the environment and the effect on human cells as well.

Acknowledgement

Authors are thankful to Department of Science and Technology (DST) and Council of Scientific and Industrial Research (CSIR), India for supporting "Nanotechnology Application Centre" under 'Nano-Mission' and 'NMITLI' scheme.

Reference

1. "Novel methods for nanoscale wire formation" edited by Prokes S. M. Prokes and Wang K. L., *MRS Bull.*, **1999**, *24*, 13.
2. Hu J, Odom T. W. and Lieber C. M., *Acc. Chem. Res.*, **1999**, 32, 435. DOI: 10.1021/ar9700365.
3. Nakamura S., *Science*, 1998, 281, 956 (*DOI: 10.1126/science.281.5379.956*).
4. Wilson, M. R., Lightbody J. H., Donaldson K., Sales J., and Stone V., *Toxicol. Appl. Pharmacol.*, 2002, 184, 172 (doi:10.1006/taap.2002.9501)
5. Sharma P K, Pandey A C, Grzegorz Zolnierkiewicz, Guskos N and Rudowicz C, J. Appl. Phys., 2009, 106, 094314. doi:10.1063/1.3256000
6. Han D, Li Y, Jia W, Adv. Mat. Lett. 2010, 1(3), 188. DOI: 10.5185/amlett.2010.7137
7. Sharma P K, Dutta R K, Kumar M, Singh P K, Pandey A C and Singh V N, IEEE Trans Nanotech, 2011, 10(1), 163. DOI: 10.1109/TNANO.2009.2037895
8. Sharma, P.K., Kumar M and Pandey A C, J. Nanopart. Res. 2011, 13, 1629. DOI: 10.1007/s11051-010-9916-3.
9. Sharma P K, Dutta R K, Pandey A C, Layek S and Verma H C, J. Magn. Magn. Mater. 2009, 321, 17, 2587. doi:10.1016/j.jmmm.2009.03.043
10. Sharma P K, Dutta R K and Pandey A C, J. Magn. Magn. Mater, 2009, 321, 3457. doi:10.1016/j.jmmm.2009.06.055
11. Sharma P K, Dutta R K and Pandey A C, J. Magn. Magn. Mater, 2009, 321, 4001. doi:10.1016/j.jmmm.2009.07.066
12. Sharma P K, Dutta R K and Pandey A C, J. Colloid Interface Sci. 2010, 345 (2), 149. doi:10.1016/j.jcis.2010.01.050
13. Nel A., Xia T., Madler L., and Li N., *Science*, 2006, 311, 622 *DOI: 10.1126/science.1114397*.
14. Strehlow W. H., Cook E. L., *J. Phys. Chem. Ref. Data*, 1973, 2, 163. doi:10.1063/1.3253115
15. Guzman K. A. D. Taylor M. R., and Banfield J. F., *Environ. Sci. Technol.*, 2006, 40, 1401. DOI: 10.1021/es0515708
16. Ohira T., Yamamoto O., Komatsu M., Sawai J. and Nakagawa Z., *J. Mater. Sci. Mater. Med.*, 2008, 19, 1407. DOI: 10.1007/s10856-007-3246
17. Wang X., Yang F., Yang W. and Yang X., *Chem. Commun*., 2007, 42, 4419. DOI: 10.1039/B708662H
18. Goodacre R., Shann B., Gilbert R. J., Timmins E. M., McGovern A. C., Alsberg B. K., Kell D. B., Logan N. A., *Anal. Chem.*, 2000, 72, 119. DOI: 10.1021/ac990661i
19. Goodacre R., Timmins E. M., Burton R., Kaderbhai N., Woodward A. M., Kell D. B., Rooney P. J., *Microbiology-UK*, 1998, 144, 1157. DOI 10.1099/00221287-144-5-1157
20. Consuelo Lo´ pez-Dı´ez E and Goodacre R., *Anal. Chem.*, 2004, 76, 585. DOI: 10.1021/ac035110d
21. Maquelin, K.; Choo-Smith, L. P.; Endtz, H. P.; Bruining, H. A.; Puppels, G. J., *J. Clin. Microbiol*, 2002, 40, 594. DOI: 10.1128/JCM.40.2.594-600.2002
22. "Surface enhanced raman spectra of escherichia coli cells using zno nanoparticles", R K Dutta, Sharma P K and Pandey A C, Digest Journal of Nanomaterials and Biostructures, 20094 (1), 83.

http://www.chalcogen.infim.ro/1RanuDutta.pdf
23. Naumann D., *Appl. Spectrosc. Rev.*, 2001, 36, 239. (DOI: 10.1081/ASR-100106157
24. Harz M., Rösch P., Peschke K.-D., Ronneberger O., Burkhardt H. and Popp J., *Analyst*, 2005, 130, 1543. DOI: 10.1039/B507715J
25. López-Díez E. C., Winder C. L., Ashton L., Currie F., and Goodacre R., *Anal. Chem.*, 2005, 77, 2901 DOI: 10.1021/ac048147m
26. Rösch P., Harz M., Schmitt M., Peschke K. D., Ronneberger O., Burkhardt H., Motzkus H. W., Lankers M., Hofer S., Thiele H., and Popp J., *Appl. Eniv. Microb.*, 2005, 71, 1626. doi:10.1128/AEM.71.3.1626-1637.2005
27. Sharma P. K., Dutta R. K., Kumar M., Singh P. K. and Pandey A. C., *J. Lumin.*, 2009, 129, 605. doi:10.1016/j.jlumin.2009.01.004
28. Brayner R., Iliou R. F., Brivois N., Djediat S., Benedetti M. F., and Fievet F., *Nanoletters*, 2006, 6 (4), 866. DOI: 10.1021/nl052326h.
29. Huang W. E., Griffiths R. I., Thompson I. P., Bailey M. J., Whiteley A. S., *Anal. Chem.*, 2004, 76, 4452. DOI: 10.1021/ac049753k
30. Xie C., Mace J., Dinno M. A., Li Y. Q., Tang W., Newton R. J., and Gemperline P. J., *Anal. Chem.*, 2005, 77, 4390. DOI: 10.1021/ac0504971
31. Britton K A, Dalterio R A, Nelson W H, Britt D, Sperry J F, *Appl. Spectrosc.*, 1988, 42, 782. http://www.opticsinfobase.org/as/abstract.cfm?URI=as-42-5-782
32. Maquelin K., Kirschner C., Choo-Smith L. P., N. Braak V D, Endtz H. P, Naumann D., Puppels G. J., *J. Microbiol. Methods*, 2002, 51, 255. doi:10.1016/S0167-7012(02)00127-6
33. Notingher I., Verrier S., Haque S., Polak J. M., Hench L. L., *Biopolymers* 2003, 72, 230. DOI: 10.1002/bip.10378
34. Dutta R K, Sharma P K, Bhargava R, Kumar N and Pandey A C, J. Phys. Chem. B, 2010, 114, 5594. DOI: 10.1021/jp1004488
35. Pupples G. J. de, Mul F. F. M., Otto C., Greve J., Robert-Nicoud M., Arndt-Jovin D. J., Jovin T. M., *Nature*, 1990, 347, 301. doi:10.1038/347301a0
36. Nijssen A., Schut T. C. B., Henle F., Caspers P. J., Hayes D. P., Neumann M. H. A., Puppels G. J., *J. Invest. Dermatol.*, 2003, 119, 64. doi:10.1046/j.1523-1747.2002.01807.x
37. Spiro T. G., Gaber B. P., *Ann Rev Biochem*, 1977, 46, 553. DOI: 10.1146/annurev.bi.46.070177.003005
38. Jeng H. A., and Swanson J., *J. EnViron. Sci. Health A Tox. Hazard Subst. EnViron. Eng.*, 2006, 41, 2699. DOI: 10.1080/10934520600966177
39. Park S., Lee Y. K., Jung M., Kim K. H., Chung N., Ahn E. K., Lim Y. and Lee K. H., *Inhal. Toxicol.*, 2007, 19, 59. doi: 10.1080/08958370701493282
40. Brunner T. J., Wick P., Manser P., Spohn P., Grass R. N., Limbach L. K., Bruinink A. and Stark W., *J. En Viron. Sci. Technol.*, 2006, 40, 4374. DOI: 10.1021/es052069i
41. Gojova A., Guo B., Kota R. S., Rutledge J. C., Kennedy I. M. and Barakat A. I., *EnViron. Health Perspect.*, 2007, 115, 403 . doi:10.1289/ehp.8497
42. Karlsson H. L., Cronholm P., Gustafsson J., and MÖller L., *Chem. Res. Toxicol.*, 2008, 21 (9), 1726. DOI: 10.1021/tx800064j
43. Padmavathy N. and Vijayaraghavan R., *Sci. Technol. Adv. Mater.*, 2008, 9, 035004. doi:10.1088/1468-6996/9/3/035004
44. Sunada K., Kikuchi Y., Hashimoto K. and Fujshima A., *Environ. Sci. Technol.*, 1998, 32, 726. DOI: 10.1021/es970860o
45. Fang M., Chen J. H., Xu X. L., Yang P. H. and Hildebrand H. F., *Int. J. Antimicrob. Agents*, 2006, 27, 513. doi:10.1016/j.ijantimicag.2006.01.008

